2010 IEEE International Conference on Robotics and Automation
Anchorage Convention District
May 3-8, 2010, Anchorage, Alaska, USA

Dynamic Object Manipulation using a Virtual Frame by a Triple Soft-Fingered Robotic Hand

Kenji Tahara, Suguru Arimoto and Morio Yoshida

Abstract— **This paper proposes a novel object manipulation method to regulate the position and attitude of an object in the task space with dynamic stability by using a triple soft-fingered robotic hand system. In our previous works, a dynamic object grasping method without use of any external sensing, called "the Blind Grasping", has been proposed. Although stable grasping in a dynamic sense has been realized by the method, a simultaneous object position and attitude control has not yet been treated, so far. In this paper, instead of using any information of the real object position and attitude, virtual data of object position and attitude are introduced by defining a virtual frame. By using the virtual information, a control signal to regulate the virtual object position and attitude without use of any external sensing is designed. The usefulness of our proposed control method even under the existence of nonholonomic rolling constraints is illustrated through a numerical simulation result.**

I. INTRODUCTION

To manipulate an object stably and dexterously by a multi-fingered robotic hand has attracted a lot of research workers in robotics. However, it is hard to realize to do because many difficulties have still now been unsolved [1–3]. One can say that one of these difficulties may come from its complicated physical interaction. Namely, the system expression of an object manipulation by the multi-fingered robotic hand is apt to become mathematically complicated and not easy to understand from the viewpoint of mechanics. It is because the system is redundant and under-actuated with many physical contact conditions such as a point, area, rolling, or sliding contact, and so on. Accordingly, many previous works related to the object manipulation have missed some complicated aspects of its dynamics, and they have been inclined to discuss it under a statical or quasi-statical standpoint [4], [5]. However, we believe that the dynamical aspects of object manipulation must be considered in order to acquire a human-like dexterous manipulation in a physical meaning [6–8]. Up to now, we have proposed a dynamic object grasping method without use of any external sensing by using a dual, or a triple soft-fingered robotic hand system, which has been based on the blind grasping methodology proposed by Arimoto *et al.* [8]. However in our previous works [9], [10], only a stability problem of grasping has been treated, but the object manipulation such as an object position and attitude control has not yet been considered.

In this paper, a novel object manipulation method is proposed in addition to the stable object grasping scheme which has been previously presented [10]. Note that a main purpose of the method proposed here is to manipulate an object not precisely, but roughly without use of any external sensing. Therefore, our control signal can be constructed only by the information available from internal sensors such as each joint angle, and angular velocity. To do this, a virtual object frame is defined at a virtual object position, which is a centroid of a triangle made by each center of fingertips. Accordingly, a virtual object position and attitude can be introduced instead of its actual data. The object manipulation method based on the virtual frame has been basically proposed by Wimböck *et al.* [11]; which did not consider the contact constraint between each fingertip and an object surface, and it has not yet guaranteed the object manipulation because the overall dynamics including interactions of each fingertip and the object surface is not taken into consideration explicitly.

In what follows, firstly overall dynamics of an object-finger system is modeled by considering physical interactions of each fingertip and an object surface. Secondly, a simple object position and attitude control signal without use of any external sensing is designed by introducing a virtual object position and attitude in the task space. Finally, a numerical simulation is conducted, and the usefulness is demonstrated through its result.

II. TRIPLE SOFT-FINGERED MODEL

A model of the triple soft-fingered robotic hand system, which consists of an index finger, a middle finger, and a thumb, used in this study is shown in Fig.1. The model presented here is the same as that has been presented in our previous work [10], but it is shown again to be convenient for the reader. The index finger and the middle finger have four D.O.F., and the thumb has five D.O.F., respectively. Hereafter, a subscript $j = i, m, t$ indicates the $\underline{i}$ndex finger, the $\underline{m}$iddle finger, and the $\underline{t}$humb respectively. Each fingertip is hemispheric and made of some sort of soft material. Assume that a grasped object is a cuboid, and the effect of gravity is ignored for the sake of simplicity for the modeling. In Fig. 1, a symbol O signifies the origin of the inertial frame. A symbol $O_{c.m.}$ is the origin of a local frame at the object mass center, and its position in the inertial frame is given by $\boldsymbol{x} \in \mathbb{R}^3$. An instantaneous rotational axis of the object

This work was partially supported by Japan Society for the Promotion of Science (JSPS), Grant-in-Aid for Scientific Research (B) (20360117) and "the Kyushu University Research Superstar Program (SSP)", based on the budget of Kyushu University allocated under President's initiative.

K. Tahara is with the Institute for Advanced Study, Kyushu University, Fukuoka 819-0395, Japan tahara@ieee.org

S. Arimoto is with the Research Organization of Science and Engineering, Ritsumeikan University, Kusatsu 525-8577, Japan arimoto@fc.ritsumei.ac.jp

K. Tahara, S. Arimoto and M. Yoshida are with the RIKEN-TRI Collaboration Center for Human-Interactive Robot Research, RIKEN, Nagoya 463-0003, Japan yoshida@nagoya.riken.jp

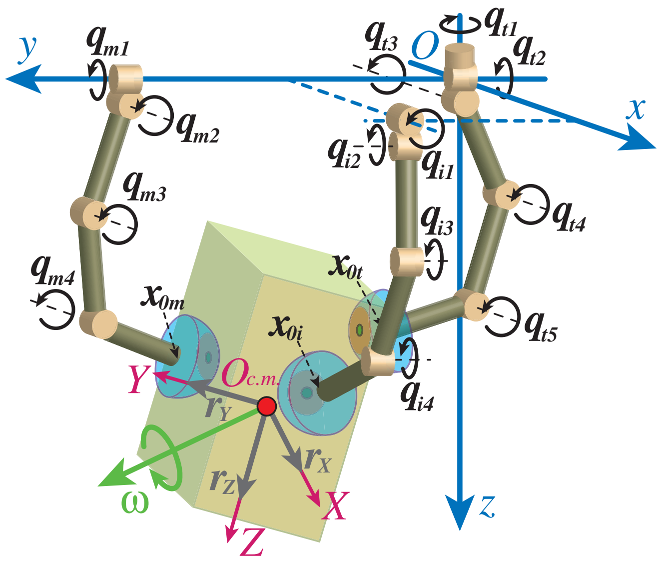

Fig. 1. Model of the triple soft-fingered robotic hand system and a grasped object

expressed by the object local frame is given by $\boldsymbol{\omega} \in \mathbb{R}^3$. Also the position of the center of each contact area in the inertial frame is denoted by $\boldsymbol{x}_j \in \mathbb{R}^3$, and the center of each fingertip in the inertial frame is by $\boldsymbol{x}_{\boldsymbol{0}j} \in \mathbb{R}^3$, respectively.

In the modeling of an object-finger system, it is important to consider a contact model between each fingertip and an object surface. Assume that each fingertip is rolling on a related object surface without slipping during movement because the shape of each fingertip is hemispheric. Also the soft fingertip makes an area contact with the object surface during manipulation. The rolling constraint with an area contact model is derived hereafter.

A. Rolling Constraint

A rolling constraint between each fingertip and an object surface can be given as a nonholonomic constraint with respect to a rolling velocity [12] in the following way:

$$\left[\begin{array}{l} (r_i - \Delta r_i)\left(-\omega_z + \boldsymbol{r_Z}^{\mathrm{T}} \boldsymbol{J}_{\boldsymbol{\Omega} i} \dot{\boldsymbol{q}}_i\right) = \dot{Y}_i \\ (r_i - \Delta r_i)\left(\omega_y - \boldsymbol{r_Y}^{\mathrm{T}} \boldsymbol{J}_{\boldsymbol{\Omega} i} \dot{\boldsymbol{q}}_i\right) = \dot{Z}_i \end{array}\right. \quad (1)$$

$$\left[\begin{array}{l} (r_m - \Delta r_m)\left(\omega_z - \boldsymbol{r_Z}^{\mathrm{T}} \boldsymbol{J}_{\boldsymbol{\Omega} m} \dot{\boldsymbol{q}}_m\right) = \dot{X}_m \\ (r_m - \Delta r_m)\left(-\omega_x + \boldsymbol{r_X}^{\mathrm{T}} \boldsymbol{J}_{\boldsymbol{\Omega} m} \dot{\boldsymbol{q}}_m\right) = \dot{Z}_m \end{array}\right. \quad (2)$$

$$\left[\begin{array}{l} (r_t - \Delta r_t)\left(-\omega_z + \boldsymbol{r_Z}^{\mathrm{T}} \boldsymbol{J}_{\boldsymbol{\Omega} t} \dot{\boldsymbol{q}}_t\right) = \dot{X}_t \\ (r_t - \Delta r_t)\left(\omega_x - \boldsymbol{r_X}^{\mathrm{T}} \boldsymbol{J}_{\boldsymbol{\Omega} t} \dot{\boldsymbol{q}}_t\right) = \dot{Z}_t \end{array}\right. \quad (3)$$

where r_j is a radius of each fingertip, Δr_j is a deformation displacement of each fingertip induced by its softness, and its definition will be shown later (see (8)). A matrix $\boldsymbol{J}_{\boldsymbol{\Omega} j}$ stands for the Jacobian matrix with respect to an attitude angular velocity of each fingertip. Moreover, $Y_i, Z_i, X_m, Z_m, X_t, Z_t$ denote each distance between each center of fingertip $\boldsymbol{x}_{\boldsymbol{0j}}$ and the object mass center $O_{c.m.}$ projected to each axis of the object local frame, and they are given in the following way:

$$\left[\begin{array}{ll} Y_i = -\boldsymbol{r_Y}^{\mathrm{T}}(\boldsymbol{x} - \boldsymbol{x}_{\boldsymbol{0}i}), & Z_i = -\boldsymbol{r_Z}^{\mathrm{T}}(\boldsymbol{x} - \boldsymbol{x}_{\boldsymbol{0}i}) \\ X_m = -\boldsymbol{r_X}^{\mathrm{T}}(\boldsymbol{x} - \boldsymbol{x}_{\boldsymbol{0}m}), & Z_m = -\boldsymbol{r_Z}^{\mathrm{T}}(\boldsymbol{x} - \boldsymbol{x}_{\boldsymbol{0}m}) \\ X_t = -\boldsymbol{r_X}^{\mathrm{T}}(\boldsymbol{x} - \boldsymbol{x}_{\boldsymbol{0}t}), & Z_t = -\boldsymbol{r_Z}^{\mathrm{T}}(\boldsymbol{x} - \boldsymbol{x}_{\boldsymbol{0}t}) \end{array}\right. \quad (4)$$

where $\boldsymbol{r_X}, \boldsymbol{r_Y}, \boldsymbol{r_Z} \in \mathbb{R}^3$ stand for mutually orthonormal vectors to define the object local frame expressed by the inertial frame. It can be represented by a rotational matrix to express an attitude of the object in the inertial frame $\boldsymbol{R}$ such that

$$\boldsymbol{R} = (\boldsymbol{r_X},\ \boldsymbol{r_Y},\ \boldsymbol{r_Z}) \in SO(3). \quad (5)$$

The rolling constraints expressed as (1) to (3) are linear with respect to each velocity vector $\dot{\boldsymbol{q}}_j, \dot{\boldsymbol{x}}, \boldsymbol{\omega}$. Therefore, they can be rewritten as Pfaffian constraints in the following forms:

$$\left[\begin{array}{l} \boldsymbol{Y}_{\boldsymbol{q}i}\dot{\boldsymbol{q}}_i + \boldsymbol{Y}_{\boldsymbol{x}i}\dot{\boldsymbol{x}} + \boldsymbol{Y}_{\boldsymbol{\omega}i}\boldsymbol{\omega} = 0 \\ \boldsymbol{Z}_{\boldsymbol{q}i}\dot{\boldsymbol{q}}_i + \boldsymbol{Z}_{\boldsymbol{x}i}\dot{\boldsymbol{x}} + \boldsymbol{Z}_{\boldsymbol{\omega}i}\boldsymbol{\omega} = 0 \end{array}\right. \quad (6)$$

$$\left[\begin{array}{l} \boldsymbol{X}_{\boldsymbol{q}j}\dot{\boldsymbol{q}}_j + \boldsymbol{X}_{\boldsymbol{x}j}\dot{\boldsymbol{x}} + \boldsymbol{X}_{\boldsymbol{\omega}j}\boldsymbol{\omega} = 0 \\ \boldsymbol{Z}_{\boldsymbol{q}j}\dot{\boldsymbol{q}}_j + \boldsymbol{Z}_{\boldsymbol{x}j}\dot{\boldsymbol{x}} + \boldsymbol{Z}_{\boldsymbol{\omega}j}\boldsymbol{\omega} = 0 \end{array}\right., \quad (j = m, t) \quad (7)$$

where $\boldsymbol{Y}_{(\boldsymbol{q},\boldsymbol{x},\boldsymbol{\omega})_i}$, $\boldsymbol{X}_{(\boldsymbol{q},\boldsymbol{x},\boldsymbol{\omega})_{(m,t)}}$, and $\boldsymbol{Z}_{(\boldsymbol{q},\boldsymbol{x},\boldsymbol{\omega})_j}$ are the constraint Jacobian matrices, respectively.

B. Deformation Displacement of the Fingertip

Each fingertip's deformation displacement toward the normal of each related object surface Δr_j is expressed in the following way:

$$\left[\begin{array}{l} \Delta r_i = (r_i + D_i) + \boldsymbol{r_X}^{\mathrm{T}}(\boldsymbol{x} - \boldsymbol{x}_{\boldsymbol{0}i}) \\ \Delta r_m = (r_m + W_m) + \boldsymbol{r_Y}^{\mathrm{T}}(\boldsymbol{x} - \boldsymbol{x}_{\boldsymbol{0}m}) \\ \Delta r_t = (r_t + W_t) - \boldsymbol{r_Y}^{\mathrm{T}}(\boldsymbol{x} - \boldsymbol{x}_{\boldsymbol{0}t}) \end{array}\right. \quad (8)$$

where D_i signifies the perpendicular distance from the center of the contact area for the index finger to the object mass center. It means the depth of the object from its mass center. Additionally, W_m and W_t denote the perpendicular distance from each center of the contact area for the middle finger and the thumb to the object mass center. Namely, $W_m + W_t$ means the width of the object.

On the othter hand, the lumped-parameterized model to give a reaction force according to a deformation displacement is introduced [7]. It is given in the following way:

$$f_j = k_{fj}\Delta r_j^2 + b_{fj}\Delta \dot{r}_j \quad (9)$$

where k_{fj} and b_{fj} denote elastic and viscosity coefficients which depend on their material and contact area, respectively.

C. Damping Effect for a Torsional Motion

A damping effect according to a torsional motion between each fingertip and the object surface is modeled [13]. The torsional damping effect can be modeled as an energy consumption function in the following way:

$$\left[\begin{array}{l} T_{\omega i} = \frac{b_i}{2}\left\|\boldsymbol{r_X}^{\mathrm{T}}(\boldsymbol{R}\boldsymbol{\omega} - \boldsymbol{J}_{\boldsymbol{\omega}i}\dot{\boldsymbol{q}}_i)\right\|^2 \\ T_{\omega j} = \frac{b_j}{2}\left\|\boldsymbol{r_Y}^{\mathrm{T}}\left(\boldsymbol{R}\boldsymbol{\omega} - \boldsymbol{J}_{\boldsymbol{\omega}j}\dot{\boldsymbol{q}}_j\right)\right\|^2, \ (j = m, t) \end{array}\right. \quad (10)$$

where $b_{i,j}$ denote a viscosity coefficient depending on its material and contact area.

D. Dynamics

An overall dynamics which takes into accout each constraint and contact model derived in previous section is given in the following way:

For the triple soft-fingered hand

$$\boldsymbol{H}_i\ddot{\boldsymbol{q}}_i + \left\{\frac{1}{2}\dot{\boldsymbol{H}}_i + \boldsymbol{S}_i\right\}\dot{\boldsymbol{q}}_i + \frac{\partial T_i}{\partial \dot{\boldsymbol{q}}_i}^{\mathrm{T}} - \boldsymbol{J_0}_i^{\mathrm{T}}\boldsymbol{r_X} f_i + (\boldsymbol{Y_{q_i}}^{\mathrm{T}}, \boldsymbol{Z_{q_i}}^{\mathrm{T}})\boldsymbol{\lambda}_i = \boldsymbol{u}_i \quad (11)$$

$$\boldsymbol{H}_m\ddot{\boldsymbol{q}}_m + \left\{\frac{1}{2}\dot{\boldsymbol{H}}_m + \boldsymbol{S}_m\right\}\dot{\boldsymbol{q}}_m + \frac{\partial T_m}{\partial \dot{\boldsymbol{q}}_m}^{\mathrm{T}} - \boldsymbol{J_0}_m^{\mathrm{T}}\boldsymbol{r_Y} f_m + (\boldsymbol{X_{q_m}}^{\mathrm{T}}, \boldsymbol{Z_{q_m}}^{\mathrm{T}})\boldsymbol{\lambda}_m = \boldsymbol{u}_m \quad (12)$$

$$\boldsymbol{H}_t\ddot{\boldsymbol{q}}_t + \left\{\frac{1}{2}\dot{\boldsymbol{H}}_t + \boldsymbol{S}_t\right\}\dot{\boldsymbol{q}}_t + \frac{\partial T_t}{\partial \dot{\boldsymbol{q}}_t}^{\mathrm{T}} + \boldsymbol{J_0}_t^{\mathrm{T}}\boldsymbol{r_Y} f_t + (\boldsymbol{X_{q_t}}^{\mathrm{T}}, \boldsymbol{Z_{q_t}}^{\mathrm{T}})\boldsymbol{\lambda}_t = \boldsymbol{u}_t \quad (13)$$

For the object

$$\boldsymbol{M}\ddot{\boldsymbol{x}} + (f_i - \lambda_{X_m} - \lambda_{X_t})\boldsymbol{r_X} + (f_m - f_t - \lambda_{Y_i})\boldsymbol{r_Y} - (\lambda_{Z_i} + \lambda_{Z_m} + \lambda_{Z_t})\boldsymbol{r_Z} = \boldsymbol{0} \quad (14)$$

$$\boldsymbol{I}\dot{\boldsymbol{\omega}} + \boldsymbol{\omega}\times\boldsymbol{I}\boldsymbol{\omega} + \sum_{j=i,m,t}\frac{\partial T_j}{\partial \boldsymbol{\omega}}^{\mathrm{T}} + \begin{pmatrix} 0 \\ Z_i \\ -Y_i \end{pmatrix} f_i + \begin{pmatrix} -Z_m \\ 0 \\ X_m \end{pmatrix} f_m + \begin{pmatrix} Z_t \\ 0 \\ -X_t \end{pmatrix} f_t + \begin{pmatrix} Z_i \\ 0 \\ -D_i \end{pmatrix}\lambda_{Y_i} + \begin{pmatrix} 0 \\ -Z_m \\ W_m \end{pmatrix}\lambda_{X_m} + \begin{pmatrix} 0 \\ -Z_t \\ -W_t \end{pmatrix}\lambda_{X_t} + \begin{pmatrix} -Y_i \\ D_i \\ 0 \end{pmatrix}\lambda_{Z_i} + \begin{pmatrix} -W_m \\ X_m \\ 0 \end{pmatrix}\lambda_{Z_m} + \begin{pmatrix} W_t \\ X_t \\ 0 \end{pmatrix}\lambda_{Z_t} = \boldsymbol{0} \quad (15)$$

where $\boldsymbol{H}_j > \boldsymbol{0}$ is an inertia matrix for each finger, $\boldsymbol{M} = \mathrm{diag}(M, M, M)$ and $M > 0$ is an object mass, $\boldsymbol{I} > \boldsymbol{0} \in \mathbb{R}^{3\times3}$ is an object inertia tensor represented by the principal axes of inertia, respectively. Also, $\boldsymbol{S}_j$ is a skew-symmetric matrix, which include Coriolis and centrifugal forces, $\lambda_{(X,Y,Z)j}$ denotes a rolling constraint force induced by each rolling constraint and $\boldsymbol{\lambda}_i = (\lambda_{Y_i}, \lambda_{Z_i})^{\mathrm{T}}$, $\boldsymbol{\lambda}_m = (\lambda_{X_m}, \lambda_{Z_m})^{\mathrm{T}}$, $\boldsymbol{\lambda}_t = (\lambda_{X_t}, \lambda_{Z_t})^{\mathrm{T}}$, f_j is a grasping force toward the normal of each contact area, and $\boldsymbol{J_0}_j$ denotes the Jacobian matrix for the velocity of the center of each fingertip $\dot{\boldsymbol{x}}_{0j}$ with respect to each joint angular velocity $\dot{\boldsymbol{q}}_j$.

III. CONTROL LAW

In this paper, we propose an object manipulation method, in which a virtual object position and attitude is controlled instead of a real position and attitude of the object. Note that the main objective of our proposed method is not to manipulate an object precisely, but to control it roughly even though the system has no external sensing device. Therefore, the control signal presented here can be constructed only by easily-available information from internal sensors such as the joint angle and angular velocity of each finger.

A. Stable Object Grasping

Firstly, a control signal to grasp an object stably is introduced. It has been proposed in our previous works [10]. It is given in the following way:

$$\boldsymbol{u_s}_j = -\frac{f_d}{\sum_{j=i,m,t} r_j}\boldsymbol{J_0}_j^{\mathrm{T}}(\boldsymbol{x_0}_j - \boldsymbol{x_M}) - \boldsymbol{C}_j\dot{\boldsymbol{q}}_j \quad (16)$$

where $\boldsymbol{x_M} \in \mathbb{R}^3$ is the virtual object position which is a centroid of a triangle made by the center of each fingertip. It is given in the following way:

$$\boldsymbol{x_M} = \frac{1}{3}\sum_{j=i,m,t}\boldsymbol{x_0}_j \quad (17)$$

Moreover, $\boldsymbol{C}_j > \boldsymbol{0}$ is a joint damping matrix for each finger and it is a positive definite diagonal matrix, and $f_d > 0$ signifies a nominal desired grasping force.

B. Regulating a Virtual Object Position

Secondly, a control signal to regulate a virtual object position is designed. It is given in the following way:

$$\boldsymbol{u_x}_j = -\frac{r_j f_d}{3\sum_{j=i,m,t} r_j}\boldsymbol{J_0}_j^{\mathrm{T}}\{\boldsymbol{K}_{px}(\boldsymbol{x_M} - \boldsymbol{x}_d) - \boldsymbol{K}_{vx}\dot{\boldsymbol{x}}_{\boldsymbol{M}}\} \quad (18)$$

where $\boldsymbol{x}_d$ denotes a desired virtual object position in the inertial frame, $\boldsymbol{K}_{px} > \boldsymbol{0} \in \mathbb{R}^{3\times3}$ and $\boldsymbol{K}_{vx} > \boldsymbol{0} \in \mathbb{R}^{3\times3}$ are position and velocity gains respectively, and they are positive definite diagonal matrices.

C. Regulating a Virtual Object Attitude

In order to regulate an object attitude without use of any external sensing as the same as the position control, we introduce a virtual object frame at the virtual object position $\boldsymbol{x_M}$. Figure 2 shows the virtual object frame $\tilde{\boldsymbol{R}} = (\tilde{\boldsymbol{r}}_{\boldsymbol{X}}, \tilde{\boldsymbol{r}}_{\boldsymbol{Y}}, \tilde{\boldsymbol{r}}_{\boldsymbol{Z}}) \in \mathbb{R}^{3\times3}$ at the virtual object position $\boldsymbol{x_M}$. To define the frame, firstly a relative position vector between the thumb's and the middle finger's center of fingertip is derived. The y axis of the virtual frame is defined by normalizing the relative position vector. It is given in the following way:

$$\tilde{\boldsymbol{r}}_{\boldsymbol{Y}} = \frac{\boldsymbol{x_0}_m - \boldsymbol{x_0}_t}{\|\boldsymbol{x_0}_m - \boldsymbol{x_0}_t\|} \in \mathbb{R}^3 \quad (19)$$

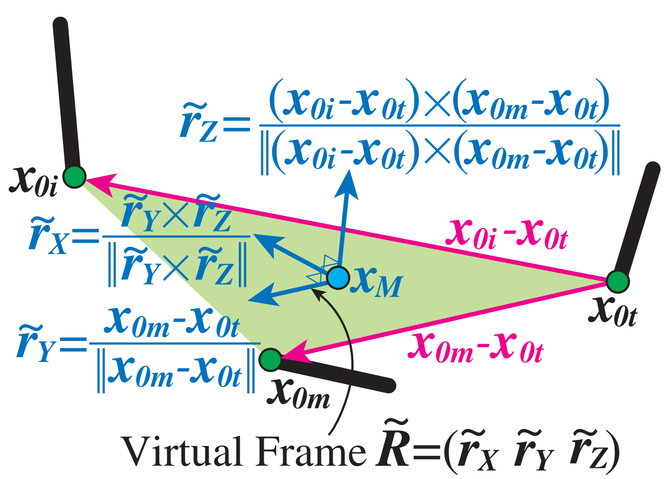

Fig. 2. Definition of the virtual object frame $\tilde{\boldsymbol{R}}$ at the virtual object position $\boldsymbol{x}_M$

Furthermore, relative position vectors between the thumb and the middle finger, and the thumb and the index finger are derived respectively. The z axis of the virtual frame is defined by taking a vector product between them and normalizing it. It is given in the following way:

$$\tilde{\boldsymbol{r}}_{\boldsymbol{Z}} = \frac{(\boldsymbol{x}_{\boldsymbol{0}m} - \boldsymbol{x}_{\boldsymbol{0}t}) \times (\boldsymbol{x}_{\boldsymbol{0}i} - \boldsymbol{x}_{\boldsymbol{0}t})}{\|(\boldsymbol{x}_{\boldsymbol{0}m} - \boldsymbol{x}_{\boldsymbol{0}t}) \times (\boldsymbol{x}_{\boldsymbol{0}t} - \boldsymbol{x}_{\boldsymbol{0}t})\|} \in \mathbb{R}^3 \tag{20}$$

Eventually, The x axis of the virtual frame is defined by taking a vector product between $\tilde{\boldsymbol{r}}_{\boldsymbol{Y}}$ and $\tilde{\boldsymbol{r}}_{\boldsymbol{Z}}$, and normalizing it. It is given in the following way:

$$\tilde{\boldsymbol{r}}_{\boldsymbol{X}} = \frac{\tilde{\boldsymbol{r}}_{\boldsymbol{Y}} \times \tilde{\boldsymbol{r}}_{\boldsymbol{Z}}}{\|\tilde{\boldsymbol{r}}_{\boldsymbol{Y}} \times \tilde{\boldsymbol{r}}_{\boldsymbol{Z}}\|} \in \mathbb{R}^3 \tag{21}$$

We are now in a position to design an object attitude control signal by using the virtual object frame defined by (19) to (20). Note that the unit vector of the virtual frame $\tilde{\boldsymbol{r}}_{\boldsymbol{X}}, \tilde{\boldsymbol{r}}_{\boldsymbol{Y}}, \tilde{\boldsymbol{r}}_{\boldsymbol{Z}} \in \mathbb{R}^3$ are mutually orthonormal, and thereby if two of these three vectors are fixed then the last one is automatically fixed. Therefore in this paper, we only use $\tilde{\boldsymbol{r}}_{\boldsymbol{X}}$ and $\tilde{\boldsymbol{r}}_{\boldsymbol{Y}}$ for the construction of the object attitude control signal. Artificial potential energies with respect to $\tilde{\boldsymbol{r}}_{\boldsymbol{X}}$ and $\tilde{\boldsymbol{r}}_{\boldsymbol{Y}}$ for the object attitude control is defined in the following way:

$$\left[\begin{array}{l} P_X = \frac{1}{2}\boldsymbol{\Delta}\tilde{\boldsymbol{r}}_{\boldsymbol{X}}^{\mathrm{T}}\boldsymbol{K}_X\boldsymbol{\Delta}\tilde{\boldsymbol{r}}_{\boldsymbol{X}} \\ P_Y = \frac{1}{2}\boldsymbol{\Delta}\tilde{\boldsymbol{r}}_{\boldsymbol{Y}}^{\mathrm{T}}\boldsymbol{K}_Y\boldsymbol{\Delta}\tilde{\boldsymbol{r}}_{\boldsymbol{Y}} \end{array}\right. \tag{22}$$

where $\boldsymbol{\Delta}\tilde{\boldsymbol{r}}_{\boldsymbol{X}} = \tilde{\boldsymbol{r}}_{\boldsymbol{X}} - \tilde{\boldsymbol{r}}_{\boldsymbol{X}d}$, $\boldsymbol{\Delta}\tilde{\boldsymbol{r}}_{\boldsymbol{Y}} = \tilde{\boldsymbol{r}}_{\boldsymbol{Y}} - \tilde{\boldsymbol{r}}_{\boldsymbol{Y}d}$, and $\tilde{\boldsymbol{r}}_{\boldsymbol{X}d}$, $\tilde{\boldsymbol{r}}_{\boldsymbol{X}d}$ signfy a desired virtual object frame which indicates a desired object attitude. Additionally, $\boldsymbol{K}_X \in \mathbb{R}^{3\times3}$ and $\boldsymbol{K}_Y \in \mathbb{R}^{3\times3}$ are positive definite diagonal matrices, respectively. Differentiating partially each artificial potential expressed as (22) with respect to each joint angle $\boldsymbol{q}_j$ yields:

$$\left[\begin{array}{l} \dfrac{\partial P_X}{\partial \boldsymbol{q}_j}^{\mathrm{T}} = \dfrac{\partial \boldsymbol{\Delta}\tilde{\boldsymbol{r}}_{\boldsymbol{X}}}{\partial \boldsymbol{q}_j}^{\mathrm{T}}\boldsymbol{K}_X\boldsymbol{\Delta}\tilde{\boldsymbol{r}}_{\boldsymbol{X}} \\ \dfrac{\partial P_Y}{\partial \boldsymbol{q}_j}^{\mathrm{T}} = \dfrac{\partial \boldsymbol{\Delta}\tilde{\boldsymbol{r}}_{\boldsymbol{Y}}}{\partial \boldsymbol{q}_j}^{\mathrm{T}}\boldsymbol{K}_Y\boldsymbol{\Delta}\tilde{\boldsymbol{r}}_{\boldsymbol{Y}} \end{array}\right. \tag{23}$$

On the other hand, differentiating $\boldsymbol{\Delta}\tilde{\boldsymbol{r}}_{\boldsymbol{X}}$ and $\boldsymbol{\Delta}\tilde{\boldsymbol{r}}_{\boldsymbol{Y}}$ with respect to the time t yields:

$$\left[\begin{array}{l} \dfrac{\mathrm{d}}{\mathrm{d}t}\boldsymbol{\Delta}\tilde{\boldsymbol{r}}_{\boldsymbol{X}} = \displaystyle\sum_{j=i,m,t}\dfrac{\partial \boldsymbol{\Delta}\tilde{\boldsymbol{r}}_{\boldsymbol{X}}}{\partial \boldsymbol{q}_j}\dot{\boldsymbol{q}}_j = \sum_{j=i,m,t}\boldsymbol{J}_{\boldsymbol{r_X}q_j}\boldsymbol{J}_{\boldsymbol{0}j}\dot{\boldsymbol{q}}_j \\ \dfrac{\mathrm{d}}{\mathrm{d}t}\boldsymbol{\Delta}\tilde{\boldsymbol{r}}_{\boldsymbol{Y}} = \displaystyle\sum_{j=i,m,t}\dfrac{\partial \boldsymbol{\Delta}\tilde{\boldsymbol{r}}_{\boldsymbol{Y}}}{\partial \boldsymbol{q}_j}\dot{\boldsymbol{q}}_j = \sum_{j=i,m,t}\boldsymbol{J}_{\boldsymbol{r_Y}q_j}\boldsymbol{J}_{\boldsymbol{0}j}\dot{\boldsymbol{q}}_j \end{array}\right. \tag{24}$$

where $\boldsymbol{J}_{\boldsymbol{r_X}q_j} \in \mathbb{R}^{3\times3}$ and $\boldsymbol{J}_{\boldsymbol{r_Y}q_j} \in \mathbb{R}^{3\times3}$ are coefficient matrices generated when differentiating $\boldsymbol{\Delta}\tilde{\boldsymbol{r}}_{\boldsymbol{X}}$ and $\boldsymbol{\Delta}\tilde{\boldsymbol{r}}_{\boldsymbol{Y}}$ with respect to the time t, and they behave as one of the Jacobian matrices. Equation (23) can be rewritten by comparing each coefficient matrics of (23) and (24) in the following way:

$$\left[\begin{array}{l} \dfrac{\partial P_X}{\partial \boldsymbol{q}_j}^{\mathrm{T}} = \boldsymbol{J}_{\boldsymbol{0}j}^{\mathrm{T}}\boldsymbol{J}_{\boldsymbol{r_X}q_j}^{\mathrm{T}}\boldsymbol{K}_X\boldsymbol{\Delta}\tilde{\boldsymbol{r}}_{\boldsymbol{X}} \\ \dfrac{\partial P_Y}{\partial \boldsymbol{q}_j}^{\mathrm{T}} = \boldsymbol{J}_{\boldsymbol{0}j}^{\mathrm{T}}\boldsymbol{J}_{\boldsymbol{r_Y}q_j}^{\mathrm{T}}\boldsymbol{K}_Y\boldsymbol{\Delta}\tilde{\boldsymbol{r}}_{\boldsymbol{Y}} \end{array}\right. \tag{25}$$

TABLE I

PARAMETERS FOR THE NUMERICAL SIMULATION

Triple robotic fingers	
1st link length l_{j1}	0.050[m]
2nd link length l_{j2}	0.030[m]
3rd link length l_{j3}	0.020[m]
1st link mass m_{j1}	0.050[kg]
2nd link mass m_{j2}	0.030[kg]
3rd link mass m_{j3}	0.020[kg]
1st link inertia $\boldsymbol{I}_{j1}$	$\mathrm{diag}(1.04, 1.04, 0.06)\times10^{-5}$[kg·m^2]
2nd link inertia $\boldsymbol{I}_{j2}$	$\mathrm{diag}(2.25, 2.25, 0.38)\times10^{-6}$[kg·m^2]
3rd link inertia $\boldsymbol{I}_{j3}$	$\mathrm{diag}(0.67, 0.67, 0.25)\times10^{-6}$[kg·m^2]
Radius of fingertip r_j	0.010[m]
Stiffness coefficient k_{fj}	3.0×10^4[N/m^2]
Damping function b_{fj}	$1000\times(2r_j\Delta r_j - \Delta r_j^2)\pi$[Ns/m^2]
Damping function b_j	$10\times(2r_j\Delta r_j - \Delta r_j^2)\pi$[Nms]

Object	
Mass m	0.05[kg]
Height h	0.035[m]
Width $W_m + W_t$	0.02[m] ($W_m = W_t = 0.01$[m])
Depth $D_i + d$	0.035[m] ($D_i = 0.0175$[m])
Inertia $\boldsymbol{I}$	$\mathrm{diag}(0.68, 1.02, 0.68)\times10^{-5}$[kg·m^2]

Desired grasping force and each gain	
f_d	1.0[N]
$\boldsymbol{K}_{px}$	$\mathrm{diag}(250, 250, 300)^{\mathrm{T}}$
$\boldsymbol{K}_{vx}$	$\boldsymbol{0}$
$\boldsymbol{K}_X$	$\mathrm{diag}(2.5, 2.5, 2.5)^{\mathrm{T}}$
$\boldsymbol{K}_Y$	$\mathrm{diag}(2.5, 2.5, 2.5)^{\mathrm{T}}$
$\boldsymbol{C}_i,\ \boldsymbol{C}_m$	$\mathrm{diag}(1.5, 1.5, 1.0, 0.8)\times10^{-2}$
$\boldsymbol{C}_t$	$\mathrm{diag}(1.8, 1.5, 1.5, 1.0, 0.8)\times10^{-2}$

Initial condition	
$\boldsymbol{q}_i$	$(0.0, -0.91, -0.83, 0.25)^{\mathrm{T}}$[rad]
$\boldsymbol{q}_m$	$(0.0, 1.09, 0.95, -0.35)^{\mathrm{T}}$[rad]
$\boldsymbol{q}_t$	$(0.0, 0.0, 2.05, -0.95, -0.35)^{\mathrm{T}}$[rad]
$\boldsymbol{x}$	(0.005, 0.025, 0.085) [m]
$\boldsymbol{\omega}$	$\boldsymbol{0}$ [rad/s]
$\boldsymbol{R}$	$\boldsymbol{I}_3$

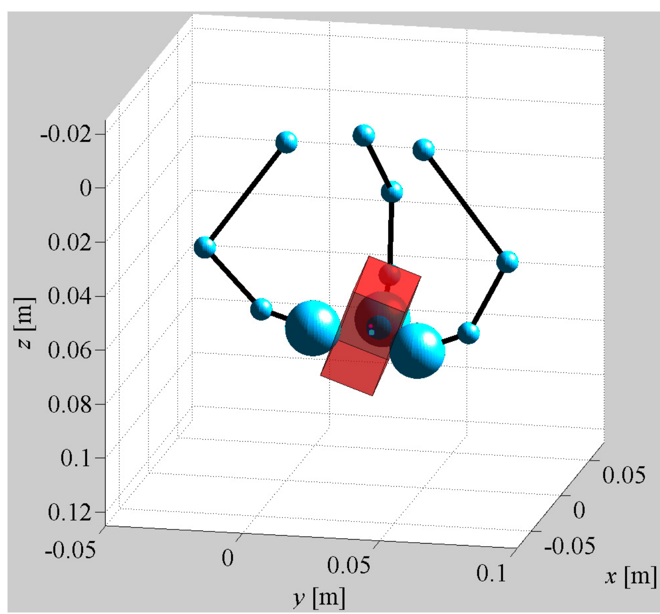

Fig. 3. Simulation graphics of the object manipulation

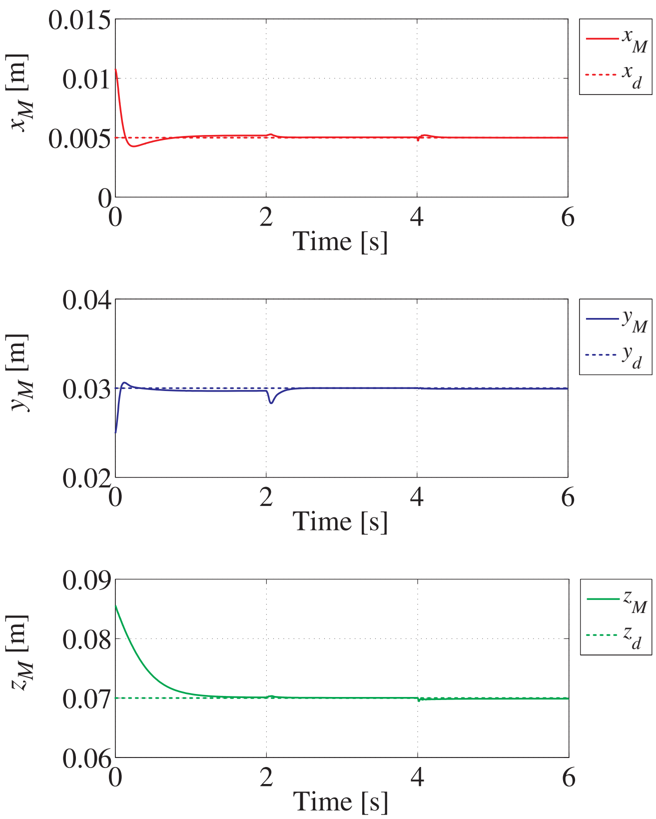

Fig. 4. Transient responses of the virtual object position $\boldsymbol{x_M}$ during manipulation

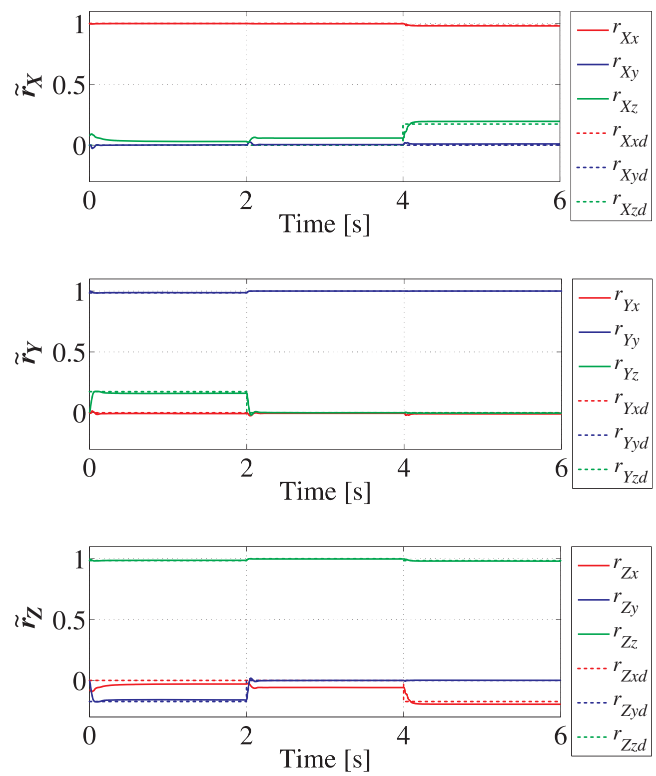

Fig. 5. Transient responses of the virtual object frame $\tilde{\boldsymbol{R}} = (\tilde{\boldsymbol{r}}_{\boldsymbol{X}}, \tilde{\boldsymbol{r}}_{\boldsymbol{Y}}, \tilde{\boldsymbol{r}}_{\boldsymbol{Z}})$ during manipulation

Hence, the control input to regulate the virtual object attitude can be constructed by using (25) in the following way:

$$\boldsymbol{u_r}_j = -\boldsymbol{J_0}_j^{\mathrm{T}}(\boldsymbol{J}_{\boldsymbol{r_X}q_j}^{\mathrm{T}}\boldsymbol{K}_X\boldsymbol{\Delta}\tilde{\boldsymbol{r}}_{\boldsymbol{X}} + \boldsymbol{J}_{\boldsymbol{r_Y}q_j}^{\mathrm{T}}\boldsymbol{K}_Y\boldsymbol{\Delta}\tilde{\boldsymbol{r}}_{\boldsymbol{Y}}) \qquad (26)$$

Eventually, the total control input to realize an object manipulation with stable grasping can be constructed by the linear summation of $\boldsymbol{u_s}_j$, $\boldsymbol{u_x}_j$ and $\boldsymbol{u_r}_j$ in the following way:

$$\boldsymbol{u}_j = \boldsymbol{u_s}_j + \boldsymbol{u_x}_j + \boldsymbol{u_r}_j. \qquad (27)$$

Note that to satisfy the stable condition in an initial state is unnecessary in our proposed controller. It is because the stable grasping controller expressed as (16) and the object manipulation controllers expressed as (18) and (26) can be independently worked, if the number of D.O.F. is enough and its configuration is adequate.

IV. NUMERICAL SIMULATION

In order to illustrate the usefulness of our proposed manipulation method, a numerical simulation is conducted here. Each parameter used in a numerical simulation is shown in Table I. In the simulation, each desired virtual object position and attitude is given as a point, and it is changed according to the time t.

Figure 3 shows a numerical simulation graphics of the object manipulation when the time $t = 1.0$ [s]. Figure 4 shows a transient response for the virtual object position $\boldsymbol{x_M}$ during manipulation. We see from these figures that the desired position is realized. Also, transient responses for each element of the unit vectors $\tilde{\boldsymbol{r}}_{\boldsymbol{X}}$,$\tilde{\boldsymbol{r}}_{\boldsymbol{Y}}$,$\tilde{\boldsymbol{r}}_{\boldsymbol{Z}}$ of the virtual object frame $\tilde{\boldsymbol{R}}$ are shown in Fig.5. We see from this figure that each element is almost converge to the desired values with several steady state errors. In our previous work [10], we have already concluded that the reaction moments around each center of contact area induced by other two fingers have to compensate in order to realize stable grasping. Therefore, we attribute these errors to the existence of these reaction moments. However, the final state of the overall system is subject to the nonlinear differential equation. Therefore, it is quite difficult to calculate an equilibrium state analytically. Namely, the relation between the object position and attitude in actual and those in virtual is not determined only in the geometrical viewpoint. We can only say at this stage that the final state of the overall system is laid on the equilibrium manifold of the total potential energy generated by the control input expressed as (27). Figures 6 and 7 show transient responses of joint angular velocities for each finger, and a velocity and an angular velocity for the object. We see from these figures that all velocities converge to zero immediately when a desired position and an attitude are realized. It indicates that a stable object grasping is realized by using our proposed controller. Furthermore, Fig. 8 shows each finger's grasping force f_j during manipulation. We see from this figure that there remain several errors against the desired grasping force f_d=1.0 [N]. It is because f_d plays a role of a nominal desired grasping force, and we have known in our previous work [10] that the real grasping force

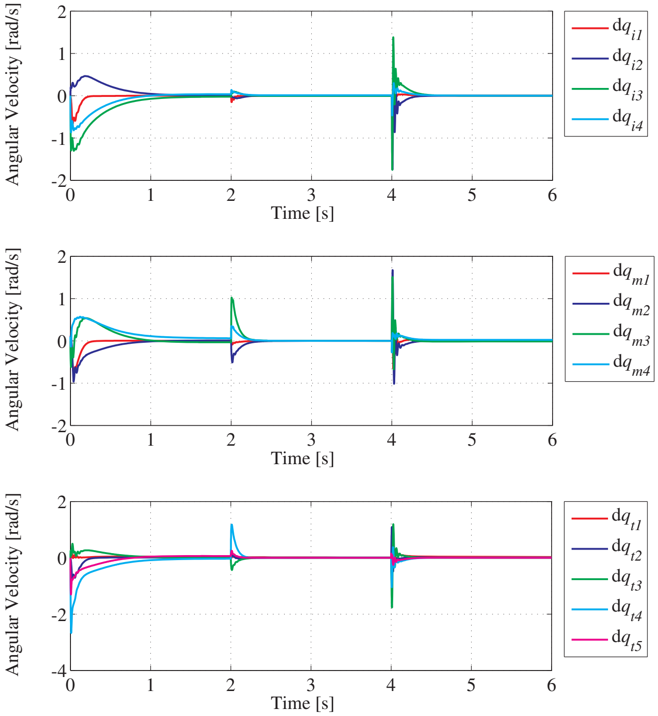

Fig. 6. Transient responses of the joint angular velocities for each finger $\dot{\boldsymbol{q}}_j$ during manipulation

is changable according to the state of the interaction between each fingertip and object surfaces. However, we can conclude that the stable object grasping is realized enough as long as each grasping force does not become zero. It means each fingertip is not detached from each object surface during manipulation. The quantity of a real grasping force should be estimated through a more detailed analysis.

V. CONCLUSION

In this paper, we proposed an object manipulation method for the triple soft-fingered robotic hand system without use of any external sensing by introducing a virtual object frame. The dynamics of the overall object-finger system, including a contact model between each fingertip and the object surface, was modeled, and the control signal to regulate a virtual object position and attitude was designed. Through a numerical simulation, we illustrated that our control scheme could realize object manipulation in that sense in a rough manner, but with stability. In our future works, we should consider some disturbances such as gravity effect, and should conduct a more detailed analysis of steady state errors. Also we have to prove the stability of the overall system.

ACKNOWLEDGMENT

This work was partially supported by Japan Society for the Promotion of Science (JSPS), Grant-in-Aid for Scientific Research (B) (20360117), and "the Kyushu University Research Superstar Program (SSP)", based on the budget of Kyushu University allocated under President's initiative.

REFERENCES

[1] K.B. Shimoga, "Robot grasp synthesis algorithms: A survey," *Int. J. Robot. Res.*, vol. 15, no. 3, pp. 230–266, 1996.
[2] A. Bicchi, "Hands for dexterous manipulation and robust grasping: A difficult road towards simplicity," *IEEE Trans. Robot. Automat.*, vol. 16, no. 6, pp. 652–662, 2000.
[3] A.M. Okamura, N. Smaby and M.R. Cutkosky, "An overview of dexterous manipulation," *Proc. IEEE Int. Conf. Robott. Automat.*, pp. 255–262, SanFrancisco, CA, 2000.
[4] M.R. Cutkosky, *Grasping and Fine Manipulation*, Kluwer Academic, Dordrecht, Netherlands; 1985.
[5] R.M. Murray, Z. Li and S.S. Sastry, *Mathematical Introduction to Robotic Manipulation*, CRC Press, Boca Raton; 1994.
[6] D. Prattichizzo and A. Bicchi, "Dynamic analysis of mobility and graspability of general manipulation system," *IEEE Trans. Robot. Automat.*, vol. 14, no. 2, pp. 241–258. 1998.
[7] S. Arimoto, P.T.A. Nguyen, H.-Y. Han and Z. Doulgeri, "Dynamics and control of a set of dual fingers with soft tips," *Robotica*, vol. 18, no. 1, pp. 71–80, 2000.
[8] S. Arimoto, "A differential-geometric approach for 2-D and 3-D object grasping and manipulation," *Annual Review in Control*, vol. 31, pp. 189–209, 2007.
[9] M. Yoshida, S. Arimoto and J.-H. Bae, "Blind grasp and manipulation of a rigid object by a pair of robot fingers with soft tips," *Proc. IEEE Int. Conf. Robot. Automat.*, pp. 4707–4714, Roma, Italy, 2007.
[10] K. Tahara, S. Arimoto and M. Yoshida, "Dynamic force/torque equilibrium for stable grasping by a triple robotic fingers system," *Proc. IEEE/RSJ Int. Conf. Intell. Robots, Syst.*, pp. 2257–2263, St. Louis, MO, 2009.
[11] T. Wimböck, C. Ott and G. Hirzinger: "Passivity-based object-level impedance control for a multifingered hand," *Proc. IEEE/RSJ Int. Conf. Intell. Robots, Syst.*, pp. 4621–4627, Beijing, China, 2006.
[12] S. Arimoto, *Control Theory of Multi-fingered Hands –A Modelling and Analytical-Mechanics Approach for Dexterity and Intelligence*, Springer; 2008.
[13] M. Yoshida, S. Arimoto and K. Tahara, "Modeling and control of a pair of robot fingers with saddle joint under orderless actuations," *Proc. IEEE Int. Conf. Robot. Automat.*, pp. 2499–2505, Kobe, Japan, 2009.

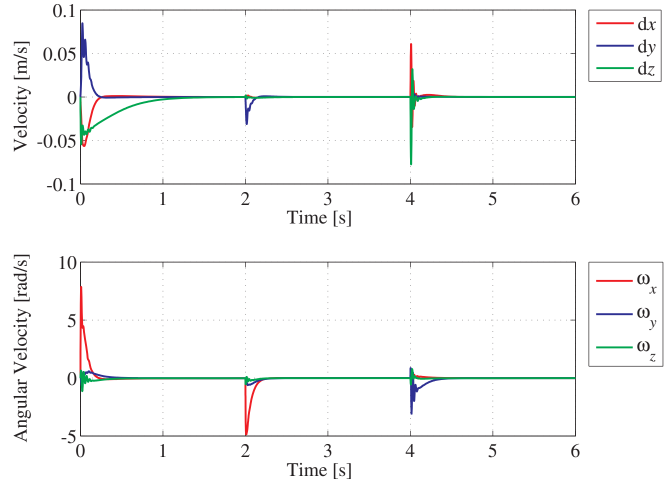

Fig. 7. Transient responses of the velocity $\dot{\boldsymbol{x}}$ and the angular velocity $\boldsymbol{\omega}$ for the object during manipulation

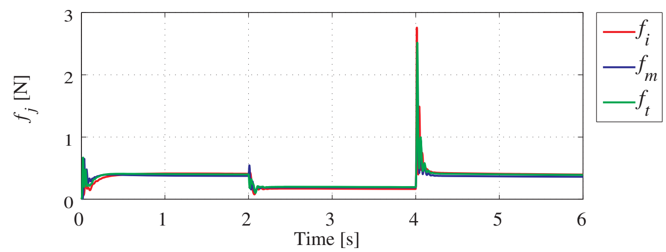

Fig. 8. Transient responses of the actual grasping force f_j during manipulation